http://dx.doi.org/10.5012/bkcs.2012.33.1.83

Alumina Templates on Silicon Wafers with Hexagonally or Tetragonally Ordered Nanopore Arrays *via* Soft Lithography

Manshik Park, Guiduk Yu, and Kyusoon Shin*

Department of Chemical and Biological Engineering, Seoul National University, Seoul 151-744, Korea
**E-mail: shin@snu.ac.kr*
Received October 15, 2011, Accepted November 3, 2011

Due to the potential importance and usefulness, usage of highly ordered nanoporous anodized aluminum oxide can be broadened in industry, when highly ordered anodized aluminum oxide can be placed on a substrate with controlled thickness. Here we report a facile route to highly ordered nanoporous alumina with the thickness of hundreds-of-nanometer on a silicon wafer substrate. Hexagonally or tetragonally ordered nanoporous alumina could be prepared by way of thermal imprinting, dry etching, and anodization. Adoption of reusable polymer soft molds enabled the control of the thickness of the highly ordered porous alumina. It also increased reproducibility of imprinting process and reduced the expense for mold production and pattern generation. As nanoporous alumina templates are mechanically and thermally stable, we expect that the simple and cost-effective fabrication through our method would be highly applicable in electronics industry.

Key Words : Imprint lithography, AAO, Self-assembly, Anodization, Electroplating

Introduction

During the recent decades, there has been an extensive range of study for manufacturing of nanomaterials due to its potential application to electronics, photonics, information storages, or filters.[1-5] Intensive efforts were put especially to the generation of nanoscopic templates with cost-efficiency, easy production and high productivity.[6-14] In this regard, self-assembly with colloidal nanoparticles, block copolymer (BCP) and anodized aluminum oxide (AAO) have been favored as well as conventional lithographic methods.[12-14] Among those methods for template production, AAO has been successfully developed as it has attractive features due to its thermal, mechanical stability together with easy fabrication of wide range of pore diameter, inter-pore distance, and length of pores.[15-17] Especially for the high aspect-ratio feature of the nanopores, AAO has been one of the good candidates that would appear as a useful template in industry as well as in research. The nanoscopic cylindrical geometry of AAO enables nanopores to pack ultra-high density and maintain anisotropy that would exhibit stronger or various properties than just a simple spherical structure.

Despite those advantages and potentials as an ultra-high density template, AAO is less widely applied than it can be, as it is not easy to prepare AAO with keeping highly ordered nanopores on an arbitrary substrate. One of the reasons for the limitations comes from the inherent formation mechanism of AAO.[17] Upon anodization of aluminum (Al), pores randomly form on surface of Al and grow up at the bottom of the pit where electric field is focused. The electrochemical oxidation process involves volume expansion, and induces stress. The balanced and appropriate degree of stress makes the pores hexagonally packed on the border between the alumina and Al. Regular pit arrays on an Al plate remain after selective removal of alumina, and the second anodization with the patterned Al results in the pores getting regularly ordered, stable, and honey-comb like hexagonal structure. In the conventional two-step anodization method,[18] at least few tens of micrometer thick AAO layer is generally sacrificed during first anodization in order to have the pores uniformly formed and hexagonally highly ordered. However, it is far from being economic and efficient to prepare few tens of micrometer thick Al on a substrate *via* physical vapor deposition methods. Moreover, it is very difficult to control the thickness of nanoporous alumina with the conventional two-step anodization method, even when tens of micrometer thick Al is placed on a substrate. As an alternative approach to two-step anodization, preparation of a regular pit array on Al surface which would guide the pore-generation was suggested by a couple of methods: block copolymer lithography, colloidal lithography or direct imprint lithography.[19-22] Placement of pre-manufactured AAO directly on a substrate could be a solution.[23] Planting electric field guide under Al layer is also reported to be valid for well ordered nanoporous AAO.[24] Among those methods, prepatterning with direct imprint lithography would be attractive, since master mold can be repeatedly used and the method itself should be simple. Moreover, as shown by Masuda and coworkers, unusual packing symmetry such as tetragonal ordering can be produced.[10] In terms of direct imprinting method on Al, however, as hard mold with nanodot patterns was proposed, fairly high pressure should be applied to imprint the nanodot patterns on flat Al. Although imprinting process could substitute for first anodization of two-step anodization method, imprinting with high pressure on Al could damage the hard master mold. Nanoporous template usually needs to be placed on a certain substrate. So, when Al needs to be loaded on a substrate, but if the

substrate is brittle, the high imprint pressure might break the substrate beneath Al.

Therefore, it requires alternatives to develop cost-effective production and mechanically stable process that could avoid damage of master pattern or substrate and make repetitive usage of the master mold available. In this study, we introduce a facile and cost-effective method to prepare submicrometer-thick AAO template with highly ordered nanopores on a Si wafer. A reusable soft mold replicated from a reusable nanoporous alumina was utilized to imprint polymer film on flat Al.[25] By dry etching of Al with imprinted polymer film on top as an etch mask, we made pits for guiding pore formation. Anodization of the prenotched Al showed that the nanopores could be highly ordered from the beginning of pore formation even with one-time anodization. Our method did not demand Al thicker than few tens of micrometer, and the thickness of the nanoporous templates can be controlled. In addition, manufacturing tetragonally arrayed nanoporous alumina can be demonstrated with taking the advantage of soft lithography. We also showed possibility that alumina template on a Si wafer could be applied as a mechanically and thermally stable ultra-high density template in electronics industry *via* barrier layer removal and electrodeposition of copper into the nanopores by employing a recently proposed method.[26]

Experimental

Manufacture of Submicrometer-thick Hexagonally Ordered Nanoporous Alumina Template. AAO template as a master mold for a polymer soft mold was prepared by conventional two-step anodization technique. Before anodization, Al foil with high purity (Goodfellow, 99.999%) was processed with chemical mechanical polishing (DS Semicon Inc.) for surface flattening. Polished Al foil was anodized at 40 V in 0.3 M oxalic acid solution at 15 °C for 12 hr; AAO was selectively etched away in chromic acid; the second anodization was carried out on the nanoscopically textured Al surface for about 85 sec under the same conditions of the first anodization. After anodization, pore diameter of AAO was widened in 0.1 M phosphoric acid solution at 30 °C, and the surface of the AAO pore walls was modified with polydimethylsiloxane, (PDMS, M_n = 5,000 g/mol, Aldrich) to make polymeric soft mold easily detached from AAO master mold without damage to the master mold and nanorods of soft mold.[27] Master mold was treated with O_2 plasma by reactive ion etcher (RIE) (RIE-3000, South Bay Technology, Inc.) for generating sufficient hydroxyl group on the surface of master mold. Afterwards, the master mold was immersed in 0.5 wt % methanol-based solution of 3-aminopropyl triethoxysilane (APTES, 99%, Aldrich) for 10 min, followed by cleaning with distilled water and methanol, and drying by N_2 blowing. Right after drying, monoglycidyl ether terminated PDMS was cast on the surface of master mold at 80 °C for 4 h for further surface modification, followed by rinsing with isopropanol. For fabricating polymer mold, polyurethane (PU)-based UV-curable prepolymer (MINS-311 RM, Minuta Tech) was poured on the surface-modified master mold, covered with transparent poly(ethylene terephthalate) (PET) substrate.[28] UV ($\lambda \sim 356 \pm 20$ nm) irradiation was performed for slight curing of the prepolymer, and the polymeric soft mold was gently separated from the master mold by physical detachment. The detached soft mold was UV-irradiated ($\lambda \sim 356 \pm 20$ nm, Minuta, MT-GJ20) for another 4 h at a dose of 10-15 mW/cm^2 for complete curing. The surface of soft mold was modified for easy release of the mold just as for the master mold.

Then, polystyrene (PS) film on Al was patterned using the polymer mold. 4-inch single polished silicon wafer (100) was purchased from Namkang Hi-Tech Co. 100 nm thick silicon oxide layer (SiO_2) was grown with dry oxidation process on Si wafer, 100 nm Titanium nitride (TiN) was sputtered on the oxide layer, and thin Al layer was deposited on the TiN layer with e-gun evaporation (600-2000 nm) at Inter-University Semiconductor Research Center (ISRC) in Seoul National University (SNU). PS (M_w = 280,000 g/mol, Aldrich) film with a thickness of ~80 nm was spun-cast on the thin Al layer (1.9 wt %, 2000 rpm). Before spin-coating of polymer thin film, evaporated Al on Si wafer was chemically mechanically polished. Thermal imprint lithography was performed in vacuum oven at 110 °C for 1.5 h by placing the polymer mold in between glass-slide supported PDMS cushion layer and glass supported PS-coated Al film on Si wafer, and tightening with clips. After thermal imprinting, the temperature of the sample was lowered first, and the soft mold was gently released from the PS film on the substrate. The sample with patterned PS layer was dry etched with Cl_2 gas by induced coupled plasma (ICP) metal etcher (Frequency~13.56 MHz, power of coil generator~600 W, power of platen generator~100 W, Cl_2 gas flow~20 sccm) in order to transfer the pattern of PS to the surface of Al film.

After the patterning, anodization of the patterned Al on the Si wafer was performed at 40 V in 0.3 M oxalic acid at 15 °C until the whole Al was oxidized. Afterwards, anodization of TiN underneath the barrier layer of AAO was further carried out for 30-150 sec after silver color dismissed. After anodization, the sample was immersed in 0.1 M phosphoric acid at 30 °C for removing cracked barrier layer of AAO, and then sequentially immersed in standard cleaning 1 (SC1) solution (NH_4OH:H_2O_2:H_2O = 1:1:5) for removing titanium oxide (TiO_2) layer that was oxidized from TiN. The TiN surface exposed through AAO template was finally electroplated in the solution mixed with 0.5 M sodium glucoheptonate ($CH_2OH(CHOH)_6COONa$), 0.1 M $CuSO_4$, and 0.1 M $ZnSO_4$.[29] To avoid electrochemical reaction on parts other than the exposed area through AAO template, samples were sealed with maskant (AC Products, inc.) before electroplating. Electroplating was performed under constant current density of 0.3 mA/cm^2. Electrodeposited AAO template was then immersed in NaOH solution (~10 wt %) in order to eliminate AAO template and obtain the metallic nanorods. Schematic procedure to hexagonally packed thin AAO without barrier layer on a substrate is given in Figure 1.

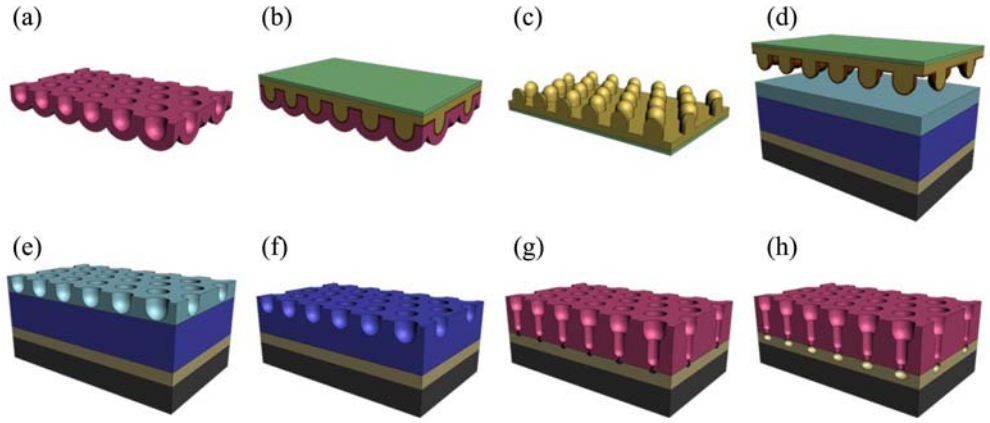

Figure 1. Schematic route to hexagonally ordered nanoporous alumina *via* soft lithography: (a) preparation of highly ordered nanoporous AAO that was used as a master mold, (b) PU-based prepolymer pouring on the surface modified master mold and partial UV-curing, (c) cured polymer soft mold, (d) thermal imprinting of PS film on Al with surface modified soft mold, (e) nanopatterned PS replicated from master mold structure, (f) surface-patterned Al through pattern transfer from the nanopatterned PS etch resist by ICP-RIE, (g) anodization of patterned Al and TiN beneath the barrier layer of AAO, and (h) AAO film on exposed TiN layer after removal of barrier layer of AAO and TiO_2. (Red: AAO, dark green: surface modified *anti*-adhesive layer, yellow green: cured PU-based polymer, green: PET substrate, sky blue: PS, blue: Al, bluish green: TiN, dark gray: Si wafer, and dark bluish green: TiO_2.)

Manufacture of Tetragonally Ordered Porous Alumina Template. In order to fabricate the tetragonally ordered porous alumina template, line patterned polymer mold was manufactured *via* similar procedure as the preparation method of hexagonally packed nanorod polymer mold. The line-patterned master mold was pretreated with the same condition for the preparation of hexagonally ordered mold. Prepolymer was poured on a line-pattern on a Si wafer with the spacing of 70 nm, and then the mold was partially cured by the irradiation of UV ($\lambda \sim 356 \pm 20$ nm, Minuta, MT-GJ20) and released from the Si wafer. The partially cured mold was completely cured by the additional irradiation of UV for another 4 h at a dose of 10-15 mW/cm^2. 80 nm thick PS film was spun-cast on an Al film or an Al coated Si wafer (with SiO_2 and TiN mid layer). Then, line pattern was thermally imprinted to the PS film on the Al film or the Al-coated Si wafer, using the line-patterned polymer mold, with the same procedure and conditions (at 110 °C for 1.5 h) used for the prepatterning of hexagonally ordered nanoporous PS film on Al. After the line-patterning of the PS film on the Al, the line pattern was transferred to Al *via* ICP-RIE (Frequency~13.56 MHz, power of coil generator~600 W, power of platen generator~100 W, Cl_2 gas flow~20 sccm). Then, PS was spun-cast on the patterned Al, and another line-patterning by thermal imprint lithography was performed normal to the long axes of previously line-patterned arrays. The line pattern was transferred to Al *via* ICP-RIE. With the two steps of line-patterning, tetragonally arrayed prepattern on the Al film or the Al-coated Si wafer was formed, and then anodization of the Al was performed at 60 V in 0.3 M oxalic acid at 15 °C. Schematic route to tetragonally ordered nanopore arrays in the anodized alumina on a Si wafer is shown in Figure 2.

Results and Discussions

For a nanoporous master mold, AAO with two-step anodization was employed. During anodization of Al, pores grow by dissolution and oxidation reactions, as a result of ion-exchange reaction between Al and electrolyte. In terms of oxide formation of Al, mechanical stress between each pore caused by volume expansion forces pores to be packed in long range; at least tens of micrometer thickness of sacrificial alumina is required for ordering of regular-sized nanopores, which corresponds to more than 10 hr process time. Etching sacrificial AAO layer selectively remains Al with

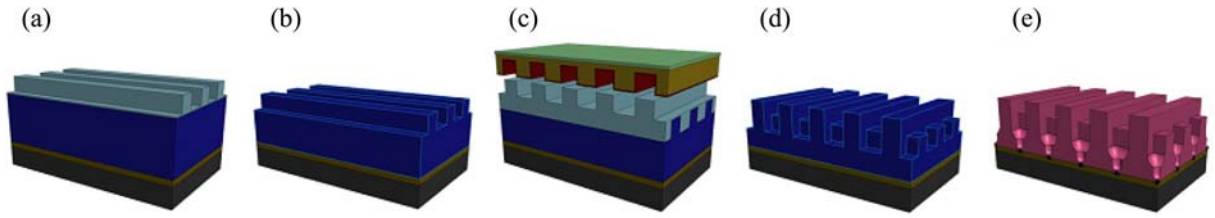

Figure 2. Schematic route to tetragonally ordered nanoporous alumina *via* soft lithography: (a) thermal imprinting of line patterns on the PS film on Al after surface modification, (b) pattern transfer from the nanopatterned PS etch resist to Al by ICP-RIE, (c) another line patterning normal to the previous line pattern *via* thermal imprinting after spin-casting on the line-patterned Al, (d) tetragonally arrayed surface-prepatterning by ICP-RIE, and (e) anodization of prepatterned Al. (Red: AAO, dark green: surface modified *anti*-adhesive layer, yellow green: cured PU-based polymer, green: PET substrate, sky blue: PS, blue: Al, bluish green: TiN, and dark gray: Si wafer.)

regular nanopit array, and second anodization using the well-ordered nanopit array Al brings out well-ordered nanoporous structure from the beginning of pore formation. A master mold in this study was fabricated by this conventional two-step anodization method. Figure 3(a) and (b) show that nanopores in the master AAO mold are well-ordered with 70-80 nm pore diameter and 100-110 nm interpore distance with 140-150 nm pore depth. Although thick nanoporous structure is favored for AAO formation or PS etch resist, considering patterning process with well patterned polymer layer as an etch resist, small aspect-ratio nanopillar of the replicated soft polymeric mold is another requirement for preventing nanopillar clamping. The aspect ratio and the diameter of nanopores were, therefore, optimized, regarding both replication process and etching process through nanoporous polymer etch resist.

For obtaining soft mold with nanopillar structure, UV-curable prepolymer was introduced *via* capillary filling in nanopores of a master mold. Before introducing the prepolymer, the surface of a master mold was modified with *anti*-adhesive thin layer, which enabled simply physical detachment of soft mold from a master mold. Most studies have been adopting chemical dissolution of AAO template to obtain metallic or polymeric nanostructures fabricated in the nanopores, which master molds are not usable for more than once. However in this study, we were able to use the master mold several times by employing simple peel-off process, without damage to the master mold, through surface treatment technique and UV-curing system. Supplementary Figure 1 represents soft mold with few defects replicated from master mold even after the eighteen time use (a), and another soft mold (b) with the opposite structure replicated from (a), showing the benefits adopting UV-curable prepolymer in this study. As a substrate of the soft mold, we made use of primer coated transparent PET film. First of all, adhesion force between PET film and PU-based UV-curable prepolymer made tight holding between them. Transparent nature of the material was advantageous during UV irradiation process. Furthermore, PET film as a substrate rendered some extent of flexibility, which was favored for peel-off process of a soft mold from a master AAO mold.

Regarding peel-off process, polymer mold was detached after slight curing of PU-based prepolymer. Experimentally, we found that clean release of nanopillars from the nanopores by physical detachment required appropriate elasticity and modulus of nanopillars as well as adhesion between PU-based polymer and PET film. With excessive curing, separation between master mold and soft mold was not easy by increased modulus of the cured-polymer and high adhesion between UV-cured polymer and master mold. Thus, detachment from a master mold after few seconds of UV-irradiation preceded complete curing for achieving hardness to stand alone without supporting structure. After peel-off process soft mold was cured enough with long time UV irradiation to ensure the adhesion between cured-polymer and PET and standing of nanopillars. Figure 3(c) and (d) represent well-ordered nanopillar structure of soft mold

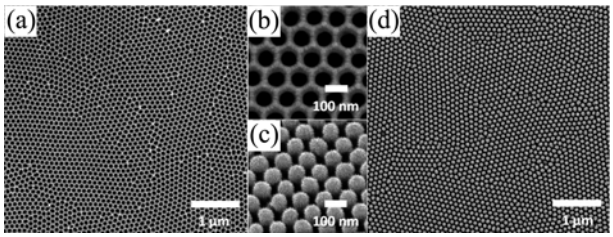

Figure 3. FE-SEM images of master mold and polymeric soft mold: (a) top view of well ordered AAO master mold and (b) magnified image of the master mold fabricated by two-step anodization. (c) 45° tilted image of soft mold and (d) top view of soft mold replicated from surface modified master mold.

replicated from a master mold, which was free of clumping between nanopillars and defects possibly resulted from detachment process.

The replicated soft mold was then used to imprint thin PS layer coated on Al/TiN/SiO_2/Si wafer with inversed, nanoporous surface pattern with residual layer as thinnest possible. The thickness of PS layer was required to be tuned in terms of two conflicting issues: prevention of random dewetting revealing Al surface (thicker film favored) and use as an etch resist of Al (thinner film favored). The PS layer was then thermally imprinted with a soft mold with pressure applied at a temperature above T_g of PS. Also in this step, the surface of a soft mold was modified with an *anti*-adhesive thin layer, considering ease of detachment of soft mold from patterned PS layer. Figure 4(a) exhibits the surface morphology of PS layer after thermal imprinting and detachment from a soft mold. As nanopillars were stiff enough and detachment was clear as much as simple.

The surface of Al with nanoporous PS etch resist was then processed by dry etching with Cl_2 gas. Anisotropic etching property of ICP-RIE and high reactivity between Al and Cl_2 gas [$Al_2 + 3Cl_2 \rightarrow Al_2Cl_6$ (volatile)] provided the possibility for fast etching at exposed Al region. Although PS etch resist was amorphous, so vulnerable in etching process, the residual layer is thin and pores were deep enough to stand the etching process to form nanopits on Al surface. Figure 4(b) is a SEM image of Al/TiN/SiO_2/Si wafer after imprinting and pattern transfer by ICP-RIE, showing that nanopits were formed on Al surface. After dry etching, the surface of etched Al became rough (Supplementary Figure 2), attributed to ICP-RIE process with Cl_2 gas. Being

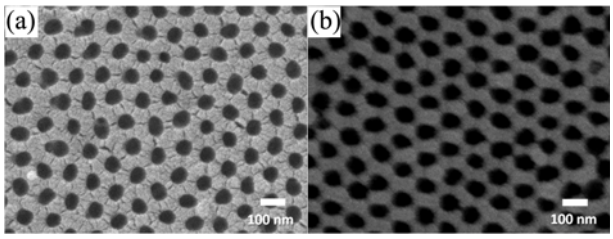

Figure 4. FE-SEM images of patterned PS and Al: (a) top view of patterned PS on an Al-coated Si wafer with TiN/SiO_2 mid layer after thermal imprinting and (b) top view of nanopit array on Al. Nanopits on Al were transferred from patterned PS to Al by ICP - RIE with Cl_2 gas.

exposed to ambient atmosphere after etching process, Cl group tethered Al surface turns into HCl in contact with moisture in air. The surface of Al was chemically etched by this acid and becomes rough. This phenomenon can be prevented by fluorine (F) substitution process, which passivates the surface of Al for corrosion in contact with ambient air. But in this study, F substitution was not carried out because the degree of roughness by the chemical reaction was considered to give negligible effect on nanopore formation guided by patterned nanopits. As a result, we could make the pattern which is the same as a master mold not only on the surface of 500 μm thick Al foil, but also evaporated thin Al on fragile TiN/SiO_2/Si wafer. Through polymer imprinting process and dry etching process the patterning of Al surface required much lower pressure than direct imprinting on Al surface with hard master mold.

Figure 5 shows nanoporous array fabricated through one-time anodization using patterned Al. When anodization was performed with Al with nanopits, nanopores started to grow from the bottoms of the pits; regularly packed nanoporous array was obtained with only one-time anodization. Selective etching on Al using nanoporous polymer etch resist brought well-ordered nanopit array, very similar to the surface with the first step AAO layer etched; it analogously

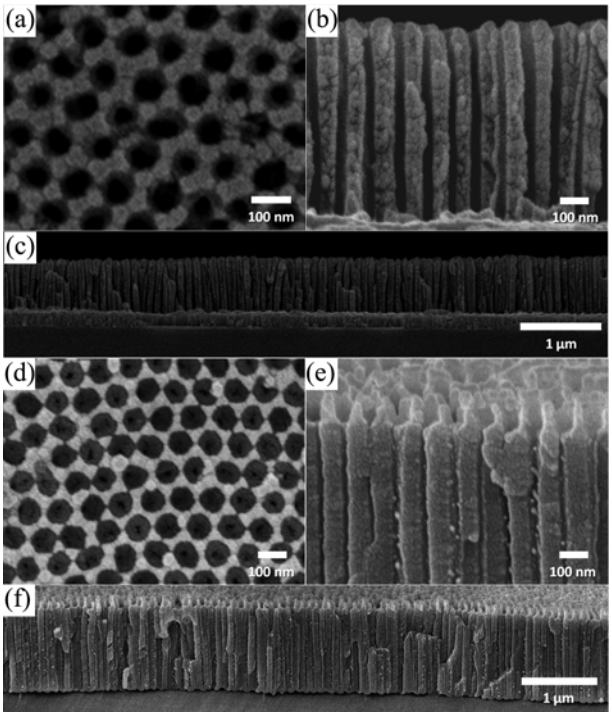

Figure 5. FE-SEM images of highly ordered thin AAO on a TiN-coated Si wafer with SiO_2 mid layer and on Al foil: (a) top view of highly ordered thin nanoporous AAO on a TiN-coated Si wafer after anodization and pore-widening, (b) magnified cross-sectional view of AAO on a TiN-coated Si wafer substrate after anodization and pore widening, (c) cross-sectional view of thin nanoporous AAO on TiN-coated Si wafer, (d) top view of highly ordered nanoporous AAO on Al foil after anodization of prenotched Al, (e) magnified cross-sectional image of AAO on Al foil, and (f) wide view of cross sectional image of AAO on Al foil.

affected local variation in electric field during anodization process. Some other studies benefiting from direct pattering techniques have also shown that the ordering and shape of nanopores can be regulated to a certain degree beyond the geometry determined by self-assembly. We confirmed that nanopores were well-ordered both thin Al layer on TiN/SiO_2/Si wafer substrate (Figure 5(a)-(c)) and thick Al foil (Figure 5(d)-(f)). It is meaningful that nanopores with regular packing can be possibly fabricated from thin Al on fragile substrate. Generally, through conventional two-step anodization process, sacrificial AAO layer for regular packing should be thicker than few tens of micrometer. In this study, however, we could obtain regularly packed nanoporous array with one-time anodization process by using pre-textured Al of thickness less than 2 μm. Moreover, highly ordered nanopores could be fabricated even on a fragile semiconducting substrate by thermal imprinting process with soft mold, which would not be easy with hard mold requiring high pressure applied for patterning surface. Combination of thermal imprint lithography (applying low pressure) and dry etching (surface texturing by selective chemical etching) was advantageous for making pre-textured Al substrate to obtain highly ordered thin AAO on fragile substrate. In Figure 5, the entrance of nanopores show some difference in size depending on the substrate, probably due to small rod-diameter difference of soft mold, thickness of coated PS layer, applied pressure for thermal imprint lithography, or degree of pore widening. Nevertheless, we made sure that those experimental parameters above did not affect the ordering of nanopores, and could not find any noticeable difference in between nanopore formation on thick Al foil and that on thin Al on TiN/SiO_2/Si wafer. During anodization of Al on TiN/SiO_2/Si wafer, we observed that the original metallic color of the surface turned into dark brown. As the evaporated Al was depleted by anodization, the color from TiN layer came out through translucent thin alumina layer. From the sudden drop in current during anodization, we could find out that the whole amount of Al is consumed and obtained nanoporous alumina array in direct contact with TiN layer. It is certain that the repetitive process would make pattern-transfer poorer. However, the soft lithography, combined with physical etching, is economic and efficient in the generation of hexagonal nanoporous alumina. The degree of hexagonal packing on the transferred alumina seems preserved, although quantitative comparison of the degree of hexagonal packing of transferred nanoporous film with the original nanoporous AAO is difficult.

Pores are hexagonally packed during the anodization to reduce the stress induced by volume expansion.[17] Since self-assembly produces hexagonal packing in general, it is difficult to have non-hexagonal arrays *via* self-assembly based method. Non-hexagonal packing of pore arrays can be achieved by other means such as direct mechanical imprinting or prepatterning with e-beam lithography. But, the mold itself can be mechanically damaged during mechanical imprinting. Also, e-beam lithography is too costly. With the current approach, however, pore arrays that are not hexa-

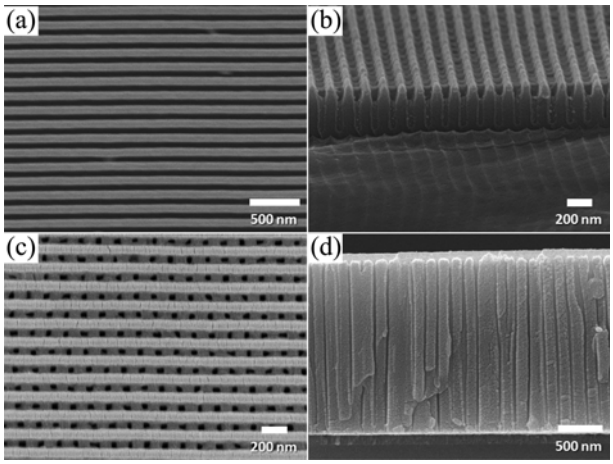

Figure 6. FE-SEM images of soft mold and tetragonally packed nanoporous alumina on an Al foil or a Si wafer: (a) line patterns on a polymer mold surface, (b) tilt view of tetragonal array of nanopores on an Al foil, and (c) top surface and (d) cross-sectional view of nanoporous alumina on a Si wafer that has tetragonally packed nanopore arrays.

gonally packed can be obtained rather efficiently and economically. In this study, as shown in Figure 6(a), a nanoscopic line-patterned polymer mold was obtained by the replication from a patterned silicon wafer. Then, the line pattern of the soft mold was imprinted on the PS film coated on the surface of Al. After thermal imprinting, Al surface with line patterned PS etch resist was etched by ICP-RIE. After the RIE etching, another line-patterning that includes imprinting and RIE etching was performed on the Al with a direction normal to the first line-patterning. Then, tetragonal array of pre-pattern was obtained on the Al surface. Upon anodization of the patterned Al, nanopore arrays that have tetragonal packing are generated, as can be seen in Figure 6(b), (c) and (d).

To show applicability as a template for obtaining metal nanorod arrays, we ran through further. Removing AAO barrier layer and exposing the conducting TiN film can make electrolyte contact with the TiN electrode and electroplating of metal nanorods available. Since the bottoms of AAO nanopores are capped, AAO is insulating. Hence, additional process is required to use it as a template for electroplating, called cap-opening process. In this study, we anodized TiN layer, making TiO_2, in order to open the barrier layer. Even in the presence of the insulating barrier layer, anodization of TiN was possible, probably because the electric field for TiN anodization would be strong enough to penetrate the barrier layer of AAO. Referring to the difference of Pilling-Bedworth ratio (Al_2O_3 ~1.65, TiO_2 ~2.87),[30,31] indicating the volume expansion upon metal oxidation, it is thought that volume expansion during the oxidation from TiN to TiO_2 brought stress at the interface between Al_2O_3 and anodized TiO_2, and damaged the barrier layer of AAO physically. Several researchers have reported uncovering process to open barrier layer.[26,32-34] Among those methods, Kim and coworkers successfully demonstrated a barrier layer-removal method, having conductive electrode at the bottom of nano-

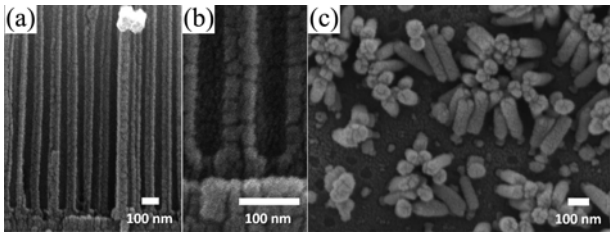

Figure 7. FE-SEM images of AAO near TiN electrode and metal nanorods on a TiN-coated Si wafer with SiO_2 mid layer: (a) cross-sectional image of barrier layer-removed AAO on a TiN-coated Si wafer with SiO_2 mid layer at the boundary between AAO and TiN, (b) magnified image of bottom of barrier-layer removed AAO, and (c) metal nanorods having bottle-shape formed by electroplating and sequential removing of AAO template.

porous alumina. In their method, electrical conducting TiN film, placed underneath of the AAO, was partially electrochemically oxidized, and then the metal oxide was chemically etched away.[26] In this study, following Kim's method, TiO_2 was selectively removed by dipping in SC1 solution, as described in the experimental section, and conductive TiN layer was exposed and used for an electrode during Cu electroplating. TiO_2 etching was performed for a short controlled time in order to reduce TiN etching. TiN also started being etched after complete chemical etching of TiO_2. Since TiN was used as an electrode, TiN should not be oxidized completely but partially. Even so, it was anodized enough to induce the crack of the AAO barrier layer. Etching with SC1 solution was carried out in mild condition at room temperature, since etching speed of TiO_2 was much faster than those of TiN and Al_2O_3 at room temperature. Figure 7(a) and (b) show the barrier layer-removed nanoporous alumina.

The specific resistivity ($R_{s,avg.}$ ~20.8) was measured after TiN was sputtered on oxidized Si wafer. Although the measured conductivity was not as high as those of materials normally used for electrodes, still it was a good candidate for both removing barrier layer of Al_2O_3 and acting itself as an electrode. For Cu electroplating, sodium glucoheptonate ($CH_2OH(CHOH)_6COONa$) was added to prevent precipitation as $Cu(OH)_2$ at pH=4.5 by forming a chelate complex with Cu ion. The solution of pH was adjusted with NaOH solution. Under constant current condition (~0.3 mA/cm^2), Cu was electrochemically deposited into nanoporous AAO template; Cu nanorods were obtained by removal of AAO membrane. From the observation of nanorods, it was again indirectly confirmed that barrier layer of AAO and anodized TiO_2 layer were successfully removed and the through-hole AAO on TiN electrode worked well as a template for obtaining metallic nanorods *via* electroplating. Cu nanorods obtained from the template-assisted electroplating are shown in Figure 7(c). Interestingly, we observed that Cu nanorods were necked at their bottoms. In the template, as can be found in Figure 7(a) and (b), the cracked and etched AAO barrier layer appeared as 'neck'. Cu nanorods look more like bottles with large caps apparently, and it implies that there is a space beneath the neck in the template. The bottom of the

neck is conjectured to be etched and enlarged due to the isotropic nature of chemical etching. As wet etchant diffuses in any direction in the TiN layer, it could dissolve etching material isotropically near the exposed area in the TiN layer. SC1 process for etching TiO_2, therefore, inevitably brought the non-uniform profile of nanopores from alumina to TiN through alumina barrier layer and TiO_2, and the shape of the etched area looks like a 'neck', so did that of Cu nanorods.

Conclusion

In summary, we introduced a facile method to obtain thin AAO templates on a substrate with highly-ordered nanopores *via* soft lithography. The current approach is effective and economic in mold manufacturing through replication of soft polymer mold from hard master mold, even enabling multiple uses of the molds. Thermal imprint lithography with soft mold facilitated patterning of Al on a fragile substrate such as Si wafer with lower pressure than adopting hard molds. Dry etching process in combination with the imprinted polymer film enabled the control of the thickness of the thin highly ordered porous template. Furthermore, other than hexagonal packing, tetragonally ordered alumina pore arrays could be generated. We could fabricate metallic nanorod arrays with AAO template through electroplating after selective elimination of barrier layer. Therefore, our approach was meaningful not only to suggest the method with cost-effectiveness, but to raise the applicability of AAO template by overcoming the limitations of anodization process.

Acknowledgments. The authors appreciate the fund support by Construction Technology Innovation Program funded by Korea Ministry of Land, Transportation and Maritime Affairs (MLTM) (09CCTI-B050566-02-000000), Basic Research Promotion Fund for new faculties (0458-20090022) by KOSEF, and Nano R&D program (2010-0019111) by the National Research Foundation of Korea. Fund support by Dongjin Semichem Co. is also acknowledged.

References

1. Kang, Y.; Walish, J. J.; Gorishnyy, T.; Thomas, E. L. *Nat. Mater.* **2007**, *6*, 957.
2. deHeer, W. A.; Bonard, J. M.; Fauth, K.; Chatelain, A.; Forro, L.; Ugarte, D. *Adv. Mater.* **1997**, *9*, 87.
3. Masuda, H.; Yamada, M.; Matsumoto, F.; Yokoyama, S.; Mashiko, S.; Nakao, M.; Nishio, K. *Adv. Mater.* **2006**, *18*, 213.
4. Thurn-Albrecht, T.; Schotter, J.; Kastle, C. A.; Emley, N.; Shibauchi, T.; Krusin-Elbaum, L.; Guarini, K.; Black, C. T.; Tuominen, M. T.; Russell, T. P. *Science* **2000**, *290*, 2126.
5. Tsou, P. H.; Sreenivasappa, H.; Hong, S.; Yasuike, M.; Miyamoto, H.; Nakano, K.; Misawa, T.; Kameoka, J. *Biosens. Bioelectron.* **2010**, *26*, 289.
6. Byun, J.; Lee, J. I.; Kwon, S.; Jeon, G.; Kim, J. K. *Adv. Mater.* **2010**, *22*, 2028.
7. Lee, K. J.; Min, S. H.; Jang, J. *Small* **2008**, *4*, 1945.
8. Massuyeau, F.; Duvail, J.; Athalin, H.; Lorcy, J.; Lefrant, S.; Wery, J.; Faulques, E. *Nanotechnology* **2009**, *20*, 155701.
9. Masuda, H.; Fukuda, K. *Science* **1995**, *268*, 1466.
10. Masuda, H.; Asoh, H.; Watanabe, M.; Nishio, K.; Nakao, M.; Tamamura, T. *Adv. Mater.* **2001**, *13*, 189.
11. Yanagishita, T.; Nishio, K.; Masuda, H. *Adv. Mater.* **2005**, *17*, 2241.
12. Krausch, G.; Magerle, R. *Adv. Mater.* **2002**, *14*, 1579.
13. Yang, S. M.; Jang, S. G.; Choi, D. G.; Kim, S.; Yu, H. K. *Small* **2006**, *2*, 458.
14. Vieu, C.; Carcenac, F.; Pepin, A.; Chen, Y.; Mejias, M.; Lebib, A.; Manin-Ferlazzo, L.; Couraud, L.; Launois, H. *Appl. Surf. Sci.* **2000**, *164*, 111.
15. Li, A.; Muller, F.; Birner, A.; Nielsch, K.; Gosele, U. *J. Appl. Phys.* **1998**, *84*, 6023.
16. Losic, D.; Lillo, M.; Losic, D., Jr. *Small* **2009**, *5*, 1392.
17. Jessensky, O.; Muller, F.; Gosele, U. *Appl. Phys. Lett.* **1998**, *72*, 1173.
18. Masuda, H.; Satoh, M. *Jpn. J. Appl. Phys., Part 2* **1996**, *35*, L126.
19. Lee, W.; Ji, R.; Ross, C. A.; Gosele, U.; Nielsch, K. *Small* **2006**, *2*, 978.
20. Lipson, A.; Comstock, D.; Hersam, M. *Small* **2009**, *5*, 2807.
21. Masuda, H.; Yamada, H.; Satoh, M.; Asoh, H.; Nakao, M.; Tamamura, T. *Appl. Phys. Lett.* **1997**, *71*, 2770.
22. Matsui, Y.; Nishio, K.; Masuda, H. *Small* **2006**, *2*, 522.
23. Maria Chong, A. S.; Tan, L. K.; Deng, J.; Gao, H. *Adv. Funct. Mater.* **2007**, *17*, 1629.
24. Nasir, M. E.; Allsopp, D. W. E.; Bowen, C. R.; Hubbard, G.; Parsons, K. P. *Nanotechnology* **2010**, *21*, 105303.
25. Chou, S. Y.; Krauss, P. R.; Renstrom, P. J. *Science* **1996**, *272*, 85.
26. Park, S. H.; Kim, S.; Lee, D. J.; Yun, S.; Khim, Z. G.; Kim, K. B. *J. Electrochem. Soc.* **2009**, *156*, K181.
27. Lee, M. J.; Lee, N. Y.; Lim, J. R.; Kim, J. B.; Kim, M.; Baik, H. K.; Kim, Y. S. *Adv. Mater.* **2006**, *18*, 3115.
28. Choi, S. J.; Yoo, P. J.; Baek, S. J.; Kim, T. W.; Lee, H. H. *J. Am. Chem. Soc.* **2004**, *126*, 7744.
29. Fujiwara, Y.; Enomoto, H. *Surf. Coat. Tech.* **1988**, *35*, 101.
30. Felhosi, I.; Habazaki, H.; Shimizu, K.; Skeldon, P.; Thompson, G.; Wood, G.; Zhou, X. *Corros. Sci.* **1998**, *40*, 2125.
31. Xu, C.; Gao, W. *Mater. Res. Innov.* **2000**, *3*, 231.
32. Foong, T. R. B.; Sellinger, A.; Hu, X. *ACS nano* **2008**, *2*, 2250.
33. Mozalev, A.; Khatko, V.; Bittencourt, C.; Hassel, A. W.; Gorokh, G.; Llobet, E.; Correig, X. *Chem. Mater.* **2008**, *20*, 6482.
34. Zhao, G. Y.; Xu, C. L.; Li, H. L. *J. Power Sources* **2007**, *163*, 1132.